Physical Gelation of Binary Mixtures of Hydrocarbons Mediated by *n*-Lauroyl-L-Alanine and Characterization of Their Thermal and Mechanical Properties

Santanu Bhattacharya* and Asish Pal

Department of Organic Chemistry, Indian Institute of Science, Bangalore 560012, Karnataka, India, and Chemical Biology Unit, JNCASR, Bangalore 560064, Karnataka, India

Received: October 30, 2007; In Final Form: December 12, 2007

Fatty acid amides, such as *n*-lauroyl-L-alanine, gelate both aliphatic and aromatic hydrocarbon solvents efficiently. In addition this compound is found to gelate the binary solvent mixtures comprised of aromatic hydrocarbon, e.g., toluene and aliphatic hydrocarbons, e.g., *n*-heptane. Scanning electron microscopy and atomic force microscopy show that the fiber thickness of the gel assembly increases progressively in the binary mixture of *n*-heptane and toluene with increasing percentage of toluene. The self-assembly patterns of the gels in individual solvents, *n*-heptane and toluene, are however different. The toluene gel consists of predominantly one type of morphological species, while *n*-heptane gel has more than one species leading to the polymorphic nature of the gel. The *n*-heptane gel is thermally more stable than the toluene gel as evident from the measurement using differential scanning calorimetry. The thermal stability of the gels prepared in the binary mixture of *n*-heptane and toluene is dependent on the composition of solvent mixture. Rheology of the gels shows that they are shear-thinning material and show characteristic behavior of soft viscoelastic solid. For the gels prepared from binary solvent mixture of toluene and *n*-heptane, with incorporation of more toluene in the binary mixture, the gel becomes a more viscoelastic solid. The time sweep rheology experiment demonstrates that the gel made in *n*-heptane has faster gel formation kinetics than that prepared in toluene.

1. Introduction

Gelation of organic solvents by low-molecular weight compounds is the subject of ever-increasing attention, not only because of the numerous applications of gels but in particular because these compounds represent a new class of materials that exhibit striking properties with respect to self-assembly phenomena.[1−4] Well-known gelling agents include, for instance, certain cholesterol and anthracene derivatives,[5−8] surfactants,[9−13] carbohydrates,[14−18] bis-urea compounds,[19−21] long-chain hydrocarbons,[22,23] amino acid derivatives,[24−31] and even metal complexes.[32] We have earlier reported that the fatty acid amides of L-alanine can gelate oil selectively from oil and water mixtures.[33] Since then several reports have appeared in literature that address this important problem of phase selective gelation.[34,35] The gelator, *n*-lauroyl-L-alanine, **1**, is a versatile gelator in gelating a variety of solvents (Chart 1). Recently, we have shown that the pockets inside a gel network can accommodate different metal nanoparticles to give rise to novel nanocomposites with improved mechanical properties.[36] A low-molecular-mass organogelator (LMOG) network can also be used as template to synthesize nanostructured materials.[36−40] Hence it is worthwhile to unravel various properties of the gels formed by **1** in various solvents or in their mixtures.

Since the gelator **1** can gelate both aromatic and aliphatic hydrocarbons, it occurred to us to see whether the binary mixture of aliphatic and aromatic solvents can also be gelated by the gelator. The mixtures of hydrocarbons are of importance in the petroleum industry due to their interesting properties, and they are studied as model oils in many occasions. Such model oils are studied for determining their emulsifying potential in terms of solubilizing resins and asphaltenes.[41−45] The extent of aromaticity of these model oils is important for stabilizing the emulsion. The asphaltenes and various resins are insoluble in light *n*-alkanes (e.g., *n*-heptane or *n*-pentane) but soluble in aromatic solvents (e.g., benzene or toluene) and hence can be separated in the form of nanoaggregates from crude oil on a preparatory scale into discrete subfractions by sequential precipitation from the binary mixtures of *n*-heptane and toluene. Also, selective separation of one type hydrocarbon from a mixture of hydrocarbons is of practical difficulty and is a challenge to the petroleum industry.

CHART 1: Molecular Structure of the Gelator 1

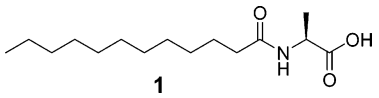

1

There are only a few reports where polymeric gelators have been used for gelating aqueous binary solvents. Appaw et al. have recently shown the effect of composition of water-*N*,*N*-dimethylacetamide in dictating the viscoelastic and microstructural behaviors of cellulose acetate gel.[46] Daniel et al. have also shown the effect of binary solvent composition of 1,2-dichloroethane and 1-chlorotetradecane in determining different phases in gels of syndiotactic polystyrene.[47] However, there is no report so far which describes the gelation of a mixture of different types of hydrocarbons by a LMOG. In this manuscript we present the gelation of single hydrocarbon solvent and mixture of miscible hydrocarbon solvents by **1** and effect of nature of hydrocarbon in controlling the self-assembly pattern. A detailed study on the thermotropic and mechanical properties of the gel network in a single hydrocarbon and binary mixture of toluene

* To whom correspondence should be addressed. E-mail: sb@orgchem.iisc.ernet.in. Phone: +91 80 2293 2664. Fax: + 91 80 2360 0529.

10.1021/jp7104715 CCC: $40.75
Published on Web 03/29/2008

and *n*-heptane has also been included. Herein, we demonstrate that the *n*-heptane gels are thermally more stable than toluene gels, while the *n*-heptane gels have less viscoelastic solidlike character than the toluene gels, and the gels prepared in the binary mixture of toluene and *n*-heptane have intermediate properties.

2. Experimental Section

2.1. Materials and Methods. The compound **1**, *n*-lauroyl-L-alanine was synthesized in high isolated yield and optical purity using a procedure reported earlier.[33,48]

2.2. Gelation Studies. Gelation tests were carried out by dissolving a known amount of the gelator in solvents taken in test tubes ($d = 8$ mm, $l = 10$ cm) upon heating. The clear solution obtained was kept at room temperature without any disturbance. Observations were recorded after 2 h, and each experiment was performed in duplicate. If a gel was formed, it was evaluated quantitatively by determining the gelation number, i.e., the mol ratio of the entrapped solvent and the gelator dictating the *maximum* number of solvent molecule that are immobilized per molecule of the gelator. For gelation of mixed solvents, different volumes of toluene and *n*-heptane were first added together to make separate mixed solvent systems. Then each mixed solvent system is added to a preweighed gelator in sample vials, and they were heated to dissolve. Upon cooling each mixture afforded a solidlike gel.

2.3. Electron Microscopy. The gels were carefully scooped onto the carbon tapes on the brass stubs and were allowed to freeze dry. Then 10-nm-thick gold films were deposited on the gels by using BAL-TEC SSD-500 sputter coater instrument. Finally the morphology of the gels was imaged on a FEI-Quanta 200 SEM operated at 5 kV.

2.4. Atomic Force Microscopy (AFM). The gels were heated to form sol, and 50 μL of the sols were deposited directly onto flat, freshly cleaved mica substrates. After the formation of stable film, AFM images were collected using a multimode instrument equipped with a NanoScope IIIa controller (Digital Instruments, Santa Barbara, California). Noncontact mode imaging was undertaken in air using silicon cantilevers from Nanosensors (Nanoworld AG, Switzerland), with cantilevers of resonance frequencies of 400−450 kHz, spring constants of 29−61 N/m, and a nominal tip radius of curvature of 5−10 nm. Images were obtained with a scan rate of 1 Hz.

2.5. X-ray Diffraction Studies (XRD). Gels of **1** (20 mg/mL) in different hydrocarbons were melted to sol, and 100 μL of the sols were individually transferred carefully on a precleaned glass slide and left to air dry for 8 h. This yielded the self-supported cast films on which measurements were performed using a Phillips X-ray diffractometer. The X-ray beam generated with a Cu anode at the wavelength of $K\alpha_1$ beam at 1.5418 Å was directed toward the film edge, and scanning was done unto a 2θ value of 12°. Data were analyzed and interpreted in terms of higher order reflections. The *hkl* values were obtained using Bragg's equation.

2.6. Differential Scanning Calorimetry (DSC). The thermotropic behaviors of the gel samples of **1** in different solvents were investigated by high-sensitivity DSC using a CSC-4100 model multicell differential scanning calorimeter (Calorimetric Sciences Corporation, Utah). Gels of **1** were prepared as mentioned above and were heated to sol, and 0.4 mL of the clear sols were carefully transferred into DSC ampules. The ampules were sealed, and the gels were allowed to set overnight at ambient conditions. The measurement was carried out in the temperature range of 10−80 °C at a scan rate of 20 °C /h. At least two consecutive heatings and coolings were performed. Baseline thermograms were obtained using same amount of the solvent in the respective DSC cells. The thermograms for the gel were obtained by subtracting the respective baseline thermogram from the sample thermogram using "CpCalc" software. From the plot of excess heat capacity vs temperature, gel-to-sol transition temperature ($T_{g\rightarrow s}$), sol-to-gel transition temperature ($T_{s\rightarrow g}$), and calorimetric enthalpies (ΔH_{cal}) of the transitions were obtained. The size of the cooperativity unit (CU) for both the melting and solidification transitions was determined using the formula $CU = (\Delta H_{vH}/\Delta H_{cal})$, where the ΔH_{vH} is the van't Hoff enthalpy, and the ΔH_{cal} is the calorimetric enthalpy. The van't Hoff enthalpy was calculated from the equation $\Delta H_{vH} = 6.9\, T_t^2/\Delta T_{1/2}$, where T_t is the the phase transition temperature (gel-to-sol transition temperature $T_{g\rightarrow s}$, sol-to-gel transition temperature $T_{s\rightarrow g}$) and $\Delta T_{1/2}$ is the full width at half-maximum of the thermogram.

2.7. Rheological Studies. For rheological characterization of the gels, an Anton Paar 100 rheometer using a cone and plate geometry (CP 25-2) with an adjustable peltier temperature-controlling system was utilized. All the measurements were done fixing the gap distance between the cone and the plate at 0.05 mm. The gel was scooped on the plate of the rheometer. The rotational flow curve (zero shear stress) measurement was performed in shear rate range of 0.01 to 100 at an interval of 25 s. The change in viscosity with shear rate can be monitored from this experiment. An oscillatory stress amplitude sweep experiment was performed at a constant oscillation frequency of 1 Hz for the strain range 0.001−100 at 20 °C. The software US-200 converted the torque measurements into either G' (the storage modulus) and G'' (the loss modulus) and represent G' and G'' with either strain or shear stress. Oscillatory frequency sweep experiments were performed in the linear viscoelastic region to ensure that calculated parameters correspond to an intact network structure. For the time sweep gel recovery experiment, the gel was melted to sol and sheared with the CP 25-2, and gel recovery (with 0.05% strain at 10 rad/s) was monitored as the build up of elastic modulus G' with time at 25 °C. Solvent evaporation was minimized by covering the rheology plate with a solvent soaked sponge chamber.

3. Results and Discussion

3.1. Gelation in a Single Hydrocarbon. The gelation efficiency of **1** toward aliphatic hydrocarbons of varying chain length and various aromatic hydrocarbon solvents was checked. For the series of increasing chain length of *n*-alkanes, although gel formation occurred rapidly (<1 min), the gel was allowed to stand for 15 min at ambient temperature to ensure complete gelation. Notably, **1** did not gelate *n*-pentane efficiently, which could in part be due to its high volatility making the gelation process compete with evaporation. As seen in Figure 1A, the gelation number goes through a maximum at $n = 7$ (where n is the number of carbon atoms in the given alkane) and thereafter remained relatively invariant. Thus we observe a requirement for an optimum lipophilicity of the solvent for efficient gelation by **1**. Also, the gels of **1** in *n*-hexane and *n*-heptane were found to be opaque in nature, while the gel prepared in *n*-hexadecane was nearly transparent. On the other hand the corresponding gels in *n*-decane and *n*-dodecane were translucent in nature. Thus an increase in optical clarity was observed upon increasing the chain length of the *n*-alkane.

The ability of **1** to gelate toxic aromatic hydrocarbon solvents was checked next. Interestingly, in contrast to the opaque optical nature of gels from *n*-alkanes, all gels formed in aromatic

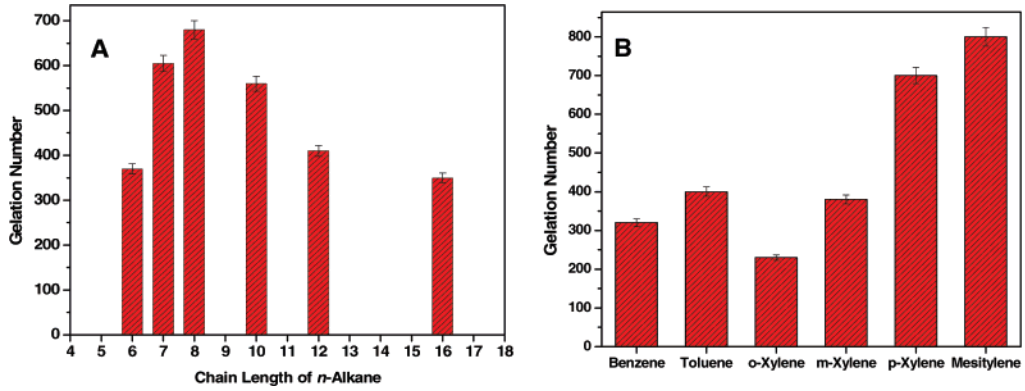

Figure 1. (A) Gelation number of **1** in different aliphatic hydrocarbons. (B) Gelation number of **1** in different aromatic hydrocarbons.

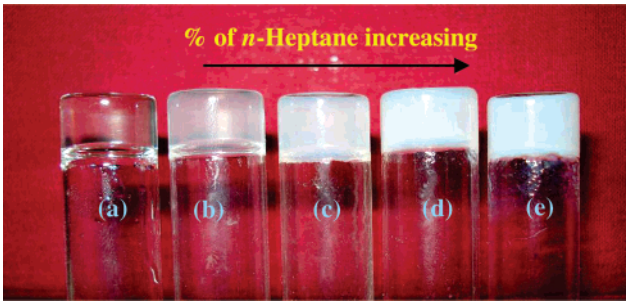

Figure 2. Gels obtained from different compositions of binary solvent mixtures of toluene and *n*-heptane with 10 mg of **1**. (a) 0% *n*-heptane, (b) 25% *n*-heptane, (c) 50% *n*-heptane, (d) 75% *n*-heptane, (e) 100% *n*-heptane in the binary mixtures of *n*-heptane and toluene.

solvents were highly transparent in nature. The gelation efficiency was found to increase with the addition of every methyl substituent in the aromatic hydrocarbon. Thus increase in gelation followed the order benzene, toluene, *p*-xylene, and mesitylene. However, a simple correlation could not be obtained because gelation efficiency also appeared to be dependent on factors such as the symmetry and hence the dipole moment of the solvent since *o*-xylene was found to be gelated poorly as compared to *p*-xylene (Figure 1B). The gel formation was faster in the case of aliphatic hydrocarbons, and the gelation was complete within ~2 min, but for aromatic hydrocarbons such as toluene, benzene, etc., the gelation kinetics was comparatively slower and took ~10−15 min to form the fully developed gels. Thus, solvent/gelator interactions[49−50] play a key role in mediating organogel formation, which ultimately determines the properties of the resulting gel.

3.2. Gelation of Binary Hydrocarbon Mixture. Binary mixtures of miscible hydrocarbon solvents are of importance for the petroleum industry. These mixtures are studied as model oils for asphaltene and resin solubilization and used for oil in emulsion tests.[41−42] Mixture of aromatic and aliphatic hydrocarbon is favored for this purpose since one can control the extent of aromatic component in of these model oils just by changing the composition of the binary mixtures. Among the binary hydrocarbon mixtures, a toluene and *n*-heptane mixture (often known as "Heptol") is commonly used in the petroleum industry.[41−45] Accordingly, the gelation tests with various mixtures of toluene and *n*-heptane were performed using **1**, and each mixture gelated quite efficiently. We found that with increasing percentage of heptane in the binary solvent mixture the opacity of the resulting gel progressively increased (Figure 2). Also the incorporation of *n*-heptane rendered the kinetics of gelation faster than that of gelation of **1** in toluene alone.

3.3. Characterization of Gels. *3.3.1. Scanning Electron Microscopy (SEM).* To discern the nature of the microstructures and morphologies present in such gels, we examined the gel samples of **1** under a scanning electron microscope. Representative SEM of the gel of **1** obtained from *n*-heptane, toluene, and their binary mixtures shows the presence of fibers of varying thickness (Figure 3). In the *n*-heptane gel a profusion of thin fibers (0.5−1.5 μm) were seen while in the toluene gels, individual fibers of regular thickness appeared to align themselves more into bundles (3−4 μm). These greater fiber alignments in the aromatic solvents might promote dominance of the fiber−fiber interactions over the fiber−solvent interactions. For gels made of a binary mixture of *n*-heptane and toluene, the bundles were seen to have intermediate thickness. As the percentage of toluene was increased progressively in the binary solvent composition, the thin individual fibers were seen to merge themselves to give rise to thick bundles of fibers.

3.3.2. AFM. We also looked at the microstuctures of the gels under AFM. In line with the SEM analysis, AFM also confirmed that gel of **1** made from *n*-heptane, toluene, and their binary mixtures possessed fibers of varying thickness (Figure 4). While in the *n*-heptane gel thinner fibers (0.4−0.6 μm) were seen, with the incorporation of toluene in the binary mixture of solvents, the thin fibers of the gel appear to merge with each other to form thicker fiber bundles (2−4 μm). Thus the fiber diameter could be controlled by the hydrocarbon compositions of the gel of **1**.

3.4. XRD. XRD of cast films of the individual gel samples has been shown to provide aggregate layer widths with consistent accuracy. Thin films of a gel prepared from (a) toluene, (b) *n*-heptane, and (c) 50% heptane in toluene of **1** were spread on precleaned glass plates and air-dried. XRD studies were performed on these self-supported cast films. A series of reflections was obtained for the gels from either solvents; the highest intensity peak being the longest d spacing (corresponds to the lowest 2θ value).

The X-ray diffraction pattern of the cast film from gel of **1** showed periodical diffraction peaks, indicating an ordered layer structure. The gel formed in toluene (Figure 5A) showed a predominantly single intense peak at 33.8 Å (80%) corresponding to the single periodicity in the structures of the aggregates. The specimen from the opaque *n*-heptane gel (Figure 5B) showed clearly the presence of two intense peaks at 33.8 (42%) and 30.9 Å (58%), giving evidence of the existence of two detectable morphs. A corresponding specimen taken from gel made from the binary solvent of 50% *n*-heptane in toluene (Figure 5C) showed two peaks corresponding to 33.6 (70%) and 30.9 Å (30%), where the morphology corresponding to d spacing of 33.6 Å was predominant. There were also very low intensity peaks at higher angles,s indicating a higher order of packing in the arrangement of gel networks (Table 1). These

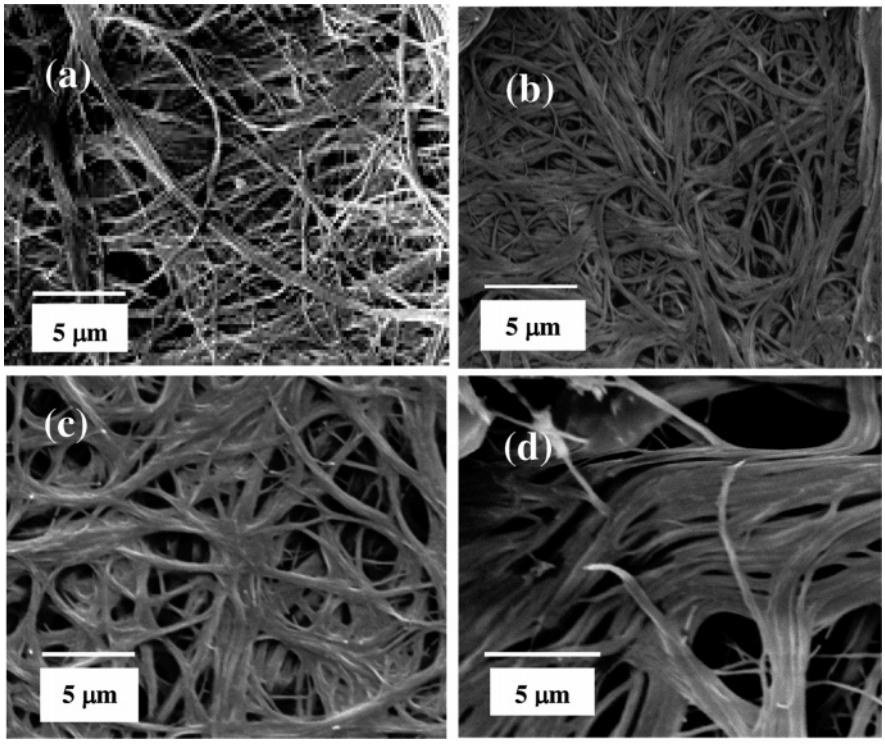

Figure 3. Scanning electron microscope images of the gels of **1** made in (a) *n*-heptane, (b) 25% toluene in *n*-heptane−toluene binary mixture, (c) 50% toluene in *n*-heptane−toluene binary mixture, and (d) toluene.

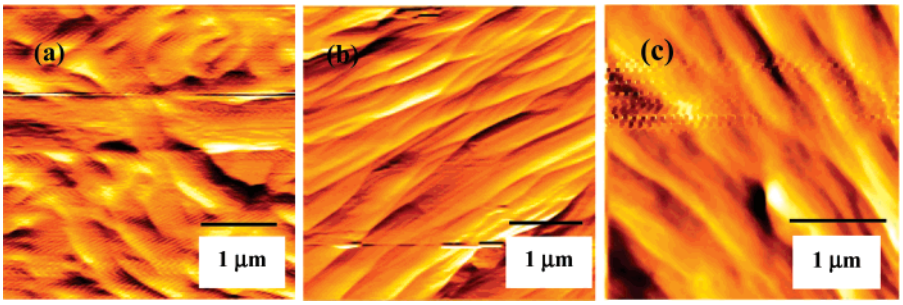

Figure 4. AFM images (noncontact mode) of the gels of **1** made in (a) *n*-heptane, (b) 50% toluene in *n*-heptane−toluene binary mixture, and (c) toluene.

peaks were in good agreement with (001) peaks of the two morphologies I and II, and suitable (*hkl*) values could be assigned to them. We observed that, with an increase in opacity of a gel from a given solvent, there was an increase in the polymorphism of the aggregates formed by the gelator in that solvent. Gels from aromatic solvents did not however show any polymorphism. The transparent optical nature of gels of aromatic hydrocarbons could be related to the absence of multiple morphs in these solvents.

3.5. Nature of Supramolecular Aggregation in Gels. Gelation is a phenomenon exhibited by molecules that have the capacity to form in three-dimensional fibrous assemblies. FTIR studies have indicated that in order to induce gelation in **1** both dimerization at the $-CO_2H$ end and intermolecular association between −NHC(O) sites are necessary.[33,48] Also, the long spacings obtained from gel of **1** in different solvents were much less than twice the molecular length calculated for gelator **1** (2.14 nm CPK model). This suggests that the gel assembly organizes itself into a repeating bilayer unit, where carboxylic acid dimers of **1** assist the packing, and the alkyl chains are tilted relative to the bilayer normal. However, it was seen that the acid dimer could itself exist in two possible conformations, one where the lauroyl chains of the acid dimer propagate in opposite directions ("transoid") (Figure 6A) and the other where they propagate in the same directions ("cisoid") (Figure 6C). In either conformation, the existence of hydrogen bonding

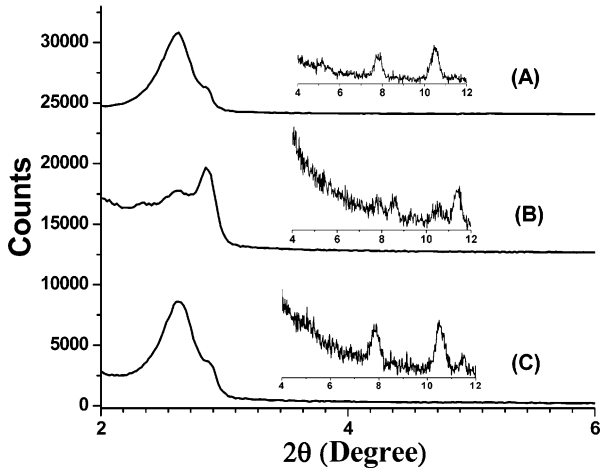

Figure 5. XRD intensities obtained from (A) toluene gel of **1**; (B) *n*-heptane gel of **1**; (C) gel of **1** in a binary solvent mixture of 37.5% *n*-heptane and 62.5% toluene. Inset shows magnification of XRD intensities in high-angle ranges. The traces are arbitrarily placed above each other to make the comparison clearer.

TABLE 1: XRD Parameters of the Gels of 1 in Different Solvents (I and II Correspond to Two Different Morphologies)

solvent	2θ (deg)	d (Å)	(hkl)
toluene	2.61	33.8	$(001)_I$
	2.85	30.9	$(001)_{II}$
	7.82	11.3	$(003)_I$
	10.49	8.4	$(004)_I$
n-heptane	2.62	33.7	$(001)_I$
	2.86	30.9	$(001)_{II}$
	7.80	11.3	$(003)_I$
	8.62	10.3	$(003)_{II}$
	10.50	8.4	$(004)_I$
	11.43	7.7	$(004)_{II}$
37.5% *n*-heptane in toluene	2.62	33.7	$(001)_I$
	2.88	30.7	$(001)_{II}$
	7.86	11.3	$(003)_I$
	10.48	8.43	$(004)_I$

between the $-CO_2H$ groups is clearly indicated, which leads to dimer formation ($d_{O-H-O} = 1.66-1.91$ Å).[48] The acid groups of the "cisoid" as well as "transoid" assembly remain in the same plane. Perpendicular to this plane the lauroyl chain containing the trans-amide linkage lies. The amide linkages form hydrogen bonds between two acid dimers, and this results in the formation of a continuous assembly ($d_{N-H-O} = 2.20-2.51$ Å). It is clear that, in both "cisoid" and "transoid" arrangements, the mode of propagation of the self-assembled structure are identical. The self-assembly of the transoid and cisoid acid dimers could give rise to two different superstructures (parts B and D of Figure 6) resulting polymorphism. It is likely that the aromatic solvents seem to prefer only one kind of acid dimer resulting in a single structure, while both forms are equally preferred in solvents such as *n*-alkanes resulting in polymorphism.

3.6. DSC of the Gel. Next we investigated the thermotropic behavior of the gels of **1** prepared in toluene, *n*-heptane, and their different binary mixtures in order to understand the thermal stability of the gels. As the gel was heated, a peak due to transition from gel to sol was observed. When the sol was cooled, it exhibited a peak due to transition from sol to gel. Repeated heating and cooling showed reproducible transition behavior indicating reversible nature of the gel assembly. The gel-to-sol melting transitions of the gels were found to be broader than the corresponding solidification transitions of sol-to-gel. The sharp exothermic peaks for the solidification transitions indicate a "discontinuous" enthalpy change, implying that the transition is first order.[51-52] The broad melting peaks for gelation suggest that the gel to sol transition is weakly first order or possibly even second order.[53] Also, the melting temperatures ($T_{g\rightarrow s}$) for gel to sol were found to be ~10-12 °C higher than the solidification temperature ($T_{s\rightarrow g}$) for sol-to-gel transition (Figure 7). This type of behavior has been observed with other LMOG-based gels also.[14,22,53-55]

When we changed the concentration of the gelator **1** in toluene, a monotonous increase in their gel-to-sol transition temperature ($T_{g\rightarrow s}$) and sol-to-gel transition temperature ($T_{s\rightarrow g}$) was observed with increasing concentration of **1** (Figure 8).When we plotted ln C vs $1/T$, it gave a straight line, the slope of which gave the molar enthalpy of gelation. The enthalpy of gel melting is 39.5 kcal/mol, which is higher than that of the enthalpy of gel formation (34.6 kcal/mol) (see SI Figure S1). This prompted us to determine the change in ΔH_{vH} and CU for both sol-to-gel formation and also for conversion of gel to sol. For both the heating and cooling process, ΔH_{vH} and CU increased monotonously (Table 2). This indicates that, with increasing concentration of the gelator, the density of the gel assembly increases to ensure participation of a greater number of gelator molecules per unit volume in the thermally induced transitions. Interestingly, the CU of the gel-to-sol transition was found to be larger than that for the sol-to-gel transition. This is not surprising as, in the gel phase, both toluene molecules and gelator molecules are immobilized, and their close proximity helps them to take part in the melting process as a collective supramolecular unit. In the sol phase however, where the gelator molecules and the toluene molecules are distributed more randomly, it can no longer participate in solidification process with a strong cooperativity. Also in the case of *n*-heptane gel of **1**, a continuous increase in their gel-to-sol transition temperature ($T_{g\rightarrow s}$) and sol-to-gel transition temperature ($T_{s\rightarrow g}$) was observed with increasing concentration of **1** (see SI Figure S2 and S3). For *n*-heptane gel of **1**, the enthalpy of gel melting is 78.1 kcal/mol, which is higher than that of the enthalpy of gel formation (61.5 kcal/mol) (see SI Figure S4). From the enthalpy values of gel melting and formation, it is clear that the *n*-heptane gel of **1** is thermally much stronger than the toluene gel of the same. Just like toluene gel, with increasing concentration of the gelator in *n*-heptane, ΔH_{vH} and CU of the assembly increased monotonously (Table 3). Noticeably, unlike the toluene gel, the CU of the sol-to-gel transition of the *n*-heptane gel is much higher than that of the gel-to-sol transition. Here, during sol-to-gel formation the aliphatic solvent molecules nucleate the gel formation by aligning themselves with the aliphatic gelator molecules, and hence the gel formation process becomes nucleation driven and cooperative in nature.

With the above information of the toluene gel of **1**, we then wanted to understand the thermotropic behavior in the gel in binary solvent mixtures of *n*-heptane and toluene. Interestingly, while the gel prepared in toluene melted at 35 °C, the gel prepared in *n*-heptane showed a melting temperature as high as 66 °C. This led us to investigate closely the behavior of different binary mixtures of *n*-heptane and toluene. With progressive increase in the percentage of *n*-heptane in the binary solvent mixture, the melting temperature ($T_{g\rightarrow s}$)went up steadily (Figure 9). Noticeably, the increase of $T_{g\rightarrow s}$ was not linear albeit it first increased gradually till 37.5% *n*-heptane incorporation in binary mixture, and then increased more abruptly with greater percentage of *n*-heptane (Figure 10). This suggested that up to 37.5% of *n*-heptane incorporation in binary mixture toluene molecules dictated the melting temperature of the gels, but further incorporation of *n*-heptane in the binary mixture rendered an abrupt increase in $T_{g\rightarrow s}$ due to increased participation of *n*-heptane. Also we found that the ΔH_{vH} and CU increased drastically with incorporation of more *n*-heptane in the binary solvent mixtures (Table 4), and thus the melting transition peak became sharper.

For cooling scan of the gel, in general, we found a sharper transition compared to the heating scan indicating that the gel formation from sol is a more cooperative phenomenon. The onset temperature ($T_{s\rightarrow g}$) of the sol to gel made in toluene was found to be ~23.1 °C, but with increasing percentage of *n*-heptane, $T_{s\rightarrow g}$ dropped first, and then it started to rise again (Figure 10). As evident from the curve, the gel formation in toluene took place at a lower temperature than in *n*-heptane. During gel formation, the molecular arrangements in the sol phase become important, and hence the compositions of the binary solvent influence $T_{s\rightarrow g}$ more than $T_{g\rightarrow s}$. At low percentages of *n*-heptane in the binary mixture, we found that gel formation onsets at lower temperature than that in pure toluene gel. Since in this range toluene molecules have a greater control on the gel behavior, a small amount of *n*-heptane incorporation

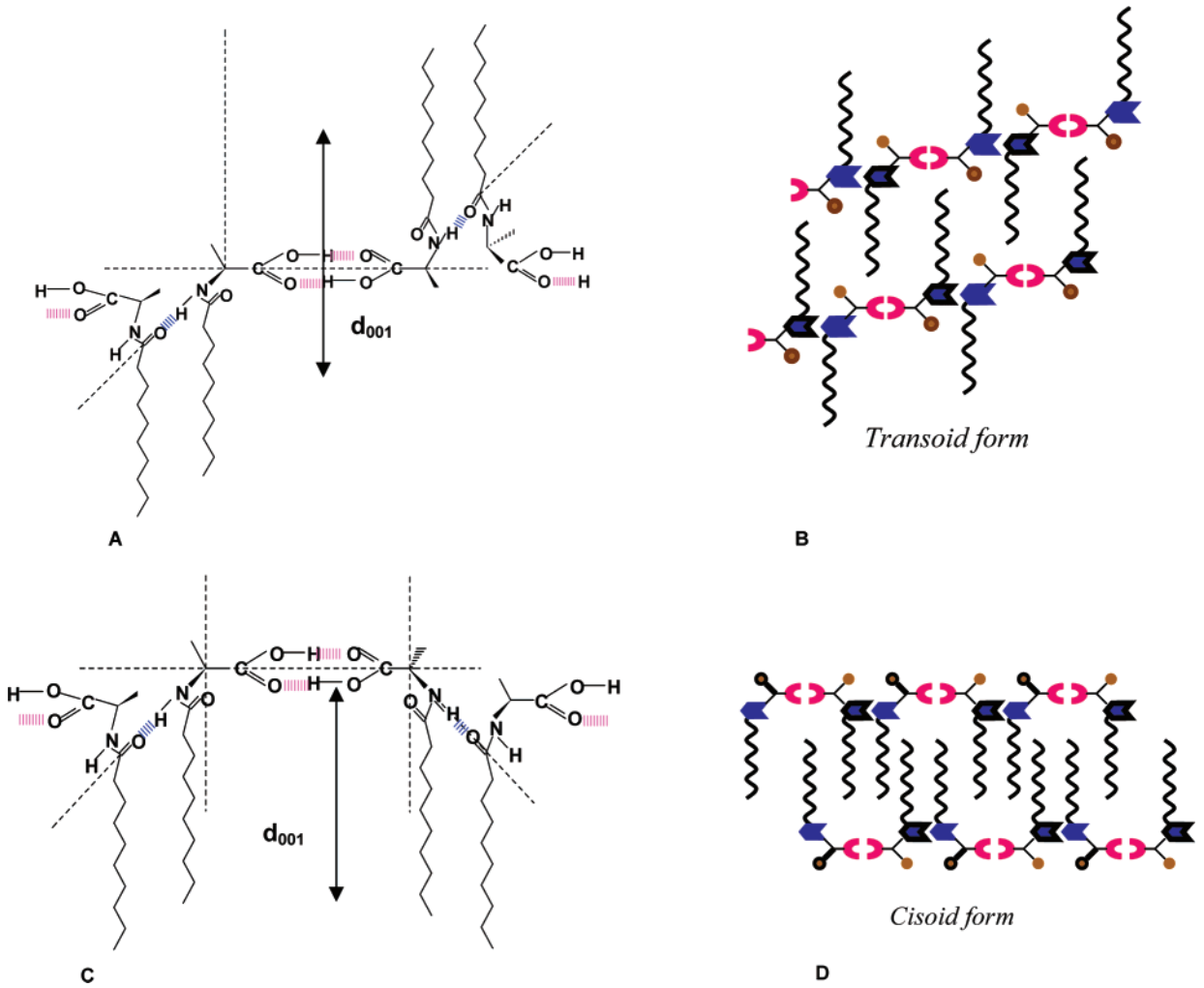

Figure 6. Three-dimensional arrangement of molecular structures of the gel assembly of **1** in (A) transoid and (C) cisoid form. Parts B and D depict the schematic representations of transoid and cisoid forms in multiple layers, respectively.

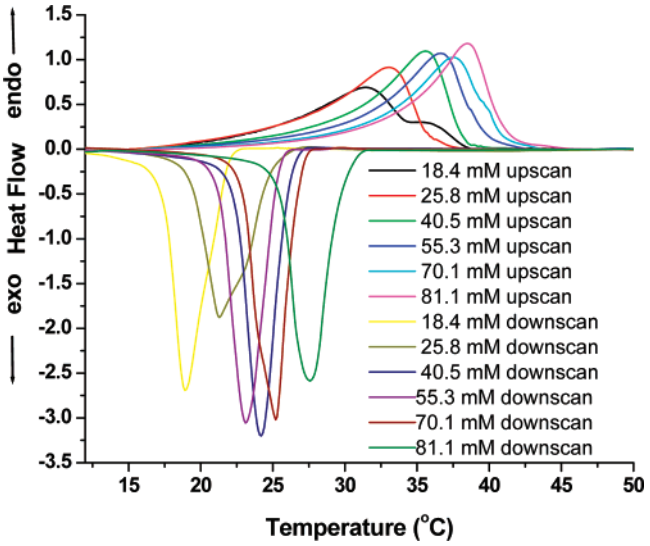

Figure 7. DSC thermograms of different concentrations of **1** in toluene.

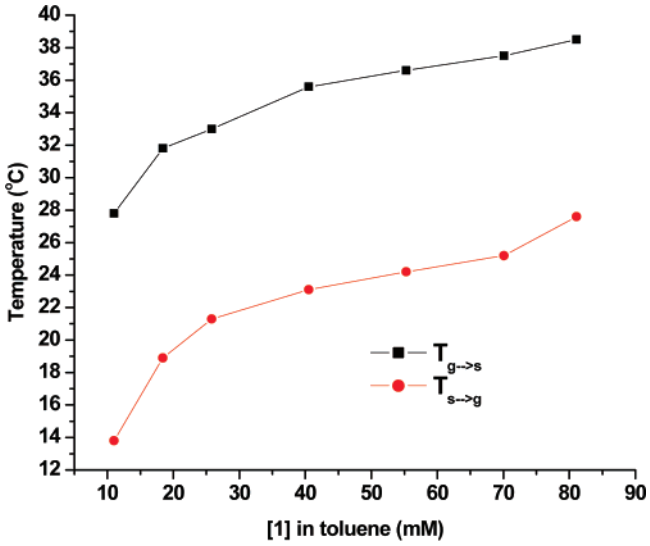

Figure 8. Plot of temperature vs concentration of **1** in toluene.

"postponed" the gel formation process compared to that in toluene gel. Above 37.5% *n*-heptane incorporation in the binary mixture, the sol-to-gel formation started to occur at higher temperatures, and the CU increased remarkably (Table 4). Also, the CU of the sol-to-gel process exceeded the CU of the gel-to-sol process indicating an active participation of *n*-heptane in the formation of gel.

3.7. Rheological Studies. Viscoelastic samples exhibit resistance to flow under applied stress. The flow behavior of the gel was measured using simple rotational flow curve experiments. With increasing the shear rate the viscosity of both *n*-heptane gel and the toluene gel decreases almost linearly (Figure 11). Even the gel from binary mixtures of these solvents behaves the same, indicating that these gels are shear thinning

TABLE 2: Summary of Thermotropic Properties of Toluene Gel of 1 at Different Concentrations (All Concentrations, Temperatures, and Enthalpies are Given in mM, °C, and kcal/mol, Respectively; Error in Temperature was ±0.5 °C)

	upscan				downscan			
concentration (mM)	$T_{g\rightarrow s}$	$\Delta H^{g\rightarrow s}{}_{cal}$	$\Delta H^{g\rightarrow s}{}_{vH}$	CU	$T_{s\rightarrow g}$	$\Delta H^{s\rightarrow g}{}_{cal}$	$\Delta H^{s\rightarrow g}{}_{vH}$	CU
18.4	31.8	6.4	929	145	18.9	7.6	893	117
25.8	33.0	7.2	1177	163	21.3	7.7	974	126
40.5	35.6	7.7	1621	210	23.1	8.4	1504	195
55.3	36.6	7.7	1711	222	24.2	8.6	1872	217
70.1	37.5	7.6	1755	230	25.2	8.1	1789	220
81.1	38.5	7.8	2081	266	27.6	8.6	1948	226

TABLE 3: Summary of Thermotropic Properties of *n*-Heptane Gel of 1 at Different Concentrations (All Concentrations, Temperatures and Enthalpies are Given in mM, °C, and kcal/mol, Respectively; Error in Temperature was ±0.5 °C)

	upscan				downscan			
concentration (mM)	$T_{g\rightarrow s}$	$\Delta H^{g\rightarrow s}{}_{cal}$	$\Delta H^{g\rightarrow s}{}_{vH}$	CU	$T_{s\rightarrow g}$	$\Delta H^{s\rightarrow g}{}_{cal}$	$\Delta H^{s\rightarrow g}{}_{vH}$	CU
7.4	64.0	8.1	7603	938	46.8	7.6	21807	2796
14.8	64.0	8.5	8056	947	48.5	9.3	22859	2822
22.1	65.0	9.1	8627	948	49.3	7.4	23036	3030
36.9	66.2	8.6	9233	1086	50.6	8.1	25492	3147
44.3	67.3	8.1	9921	1224	52.4	9.7	32834	3385

TABLE 4: Summary of Thermotropic Properties of Gel of 1 in *n*-Heptane−Toluene Binary Solvents (All Concentrations, Temperatures, and Enthalpies are Given in mM, °C, and kcal/mol, Respectively; Error in Temperature was ±0.5 °C)

	upscan				downscan			
% of *n*-heptane	$T_{g\rightarrow s}$	$\Delta H^{g\rightarrow s}{}_{cal}$	$\Delta H^{g\rightarrow s}{}_{vH}$	CU	$T_{s\rightarrow g}$	$\Delta H^{s\rightarrow g}{}_{cal}$	$\Delta H^{s\rightarrow g}{}_{vH}$	CU
0	35.6	7.7	1621	210	23.1	8.4	1504	195
12.5	37.7	8.1	1752	216	20.0	7.6	986	130
25	41.6	8.4	1953	232	18.5	8.1	1010	124
37.5	43.6	8.1	2432	300	23.4	8.3	3524	424
50	49.1	8.6	4023	468	38.8	9.3	4813	517
75	57.4	9.5	6653	700	49.5	10.0	9403	940
100	66.3	8.6	9724	1130	52.2	9.7	31336	3230

materials. In all the cases, the gels were shear thinned with a scaling decay $\eta \propto (d\gamma/dt)^{-0.97}$. The viscosity follows a sharp decay with a slope approaching −1 is exhibiting a viscoelastic solidlike behavior of this class of gels.[56]

In an oscillatory amplitude sweep experiment, results reported (a) G' or the storage modulus representing the ability of the deformed material to restore its original geometry and (b) G'' or the loss modulus, representing the tendency of a material to flow under stress. For viscoelastic materials like gels, G' is an order of magnitude greater than G'', demonstrating the dominant elastic behavior of the system. The yield stress (σ_y), refers to the applied stress above which the gel starts to flow. In other words, the property of the gel changes from a dominant elastic solidlike behavior to a dominant viscous−liquid-like behavior. Usually this point is determined by measuring the stress value at which G'' becomes larger than G' (in a so-called stress amplitude sweep experiment). Each gel has its own particular σ_y according to its strength or rigidity to an oscillating stress.[57−60]

The gel made in *n*-heptane from **1** succumbed to the applied stress and began to flow at about 23 Pa, whereas the gel made in toluene from **1** at identical concentration started to flow under applied stress at about 155 Pa (see SI, Figure S5). Therefore the toluene gel of **1** is more viscoelastic solidlike than gel of that gelator prepared in *n*-heptane. When the gelator concentration was increased in toluene, the G'/G'' and G' also progressively increased, indicating a gradual increase in viscoelastic solidlike behavior for the gels (see SI, Figure S6). To verify the power law behavior of gel, $G' \propto c^m$, logarithmic plot of storage modulus of gel vs gelator concentration was used to get the value of m (see SI, Figure S7). The yield stress (σ_y)

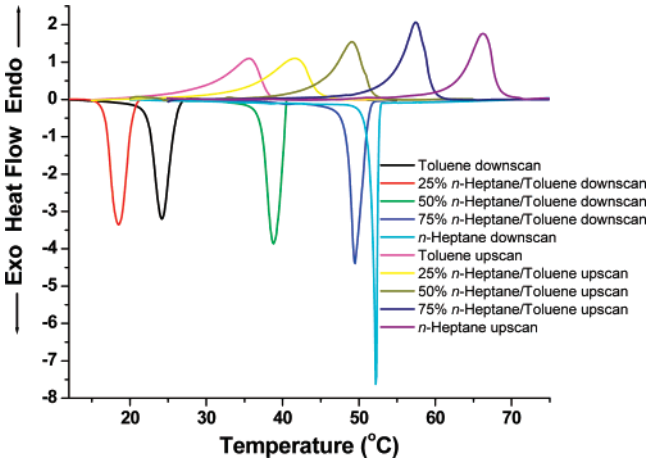

Figure 9. DSC thermograms of gels of **1** (40.5 mM) made in different compositions of binary solvents of *n*-heptane and toluene.

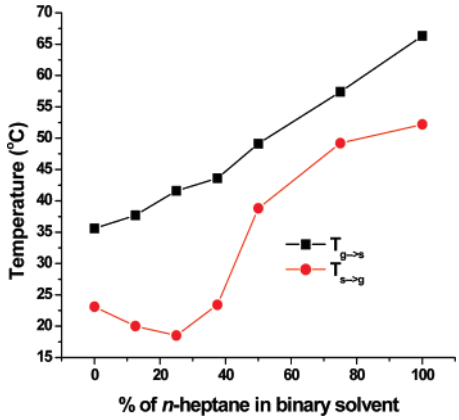

Figure 10. Plots of temperature vs percentage of *n*-heptane in binary solvent mixtures of *n*-heptane and toluene in the gels made with 40.5 mM of **1**.

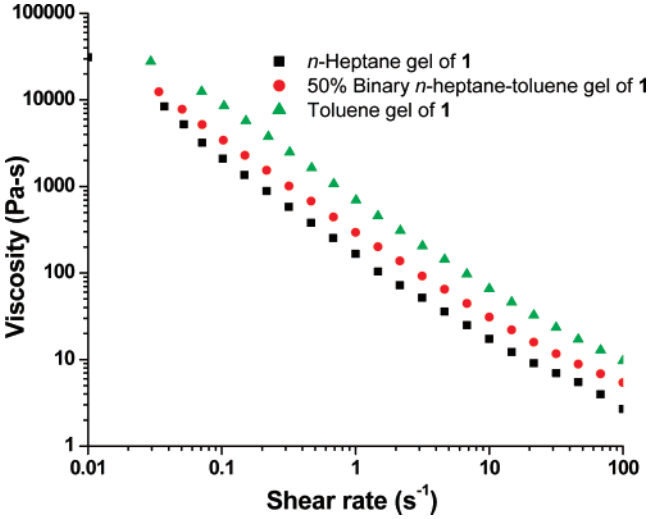

Figure 11. A typical flow curve measurement of gels made in toluene, *n*-heptane, and 50% binary mixture of *n*-heptane−toluene with 81 mM of **1**.

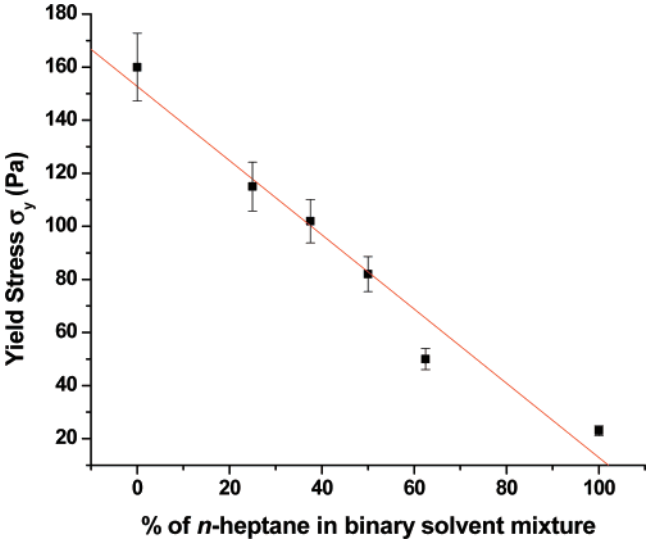

Figure 12. Plot of yield stress vs percentage of *n*-heptane in binary solvent mixture of *n*-heptane and toluene in the gels made with 81 mM of **1**.

also increased with the gelator concentration, and the magnitude was proportional to the elastic modulus and scaled as the power of the gelator concentration ($\sigma_y \propto c^n$) (see SI, Figure S8). The values of the exponents (*m* and *n*) are 2.25 and 2.33, respectively, which is in good agreement with the reported values for low molecular mass gelling agents.[61−63]

Next we examined the rheological behavior of gels prepared from binary mixtures of toluene and *n*-heptane. In these mixtures also nearly a linear decrease in yield stress value was observed with the increase in the percentage of *n*-heptane in the binary solvent mixture (Figure 12). XRD studies have shown that the gels prepared in *n*-heptane consist of more than one type of morphs in the gels. It is possible that different morphs slip over each other under applied mechanical stress, leading to manifestation of a less rigid structure of gels in *n*-heptane. Also, in line with the SEM observation, gels in aliphatic solvent have higher fiber−solvent interactions, which render them highly solvated. Hence the *n*-heptane gel is less viscoelastic solidlike though they are thermally more stable than the toluene gel.

Gels were subjected to frequency sweep in which an initial stress of 5 Pa was allowed to adjust to a constant strain of 0.001.

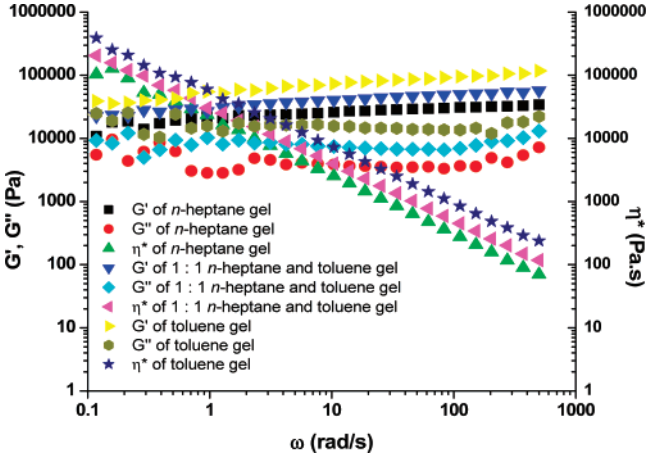

Figure 13. Typical frequency sweep experiments of the gels made in toluene, *n*-heptane, and 1:1 binary mixture of *n*-heptane−toluene with 81 mM of **1**.

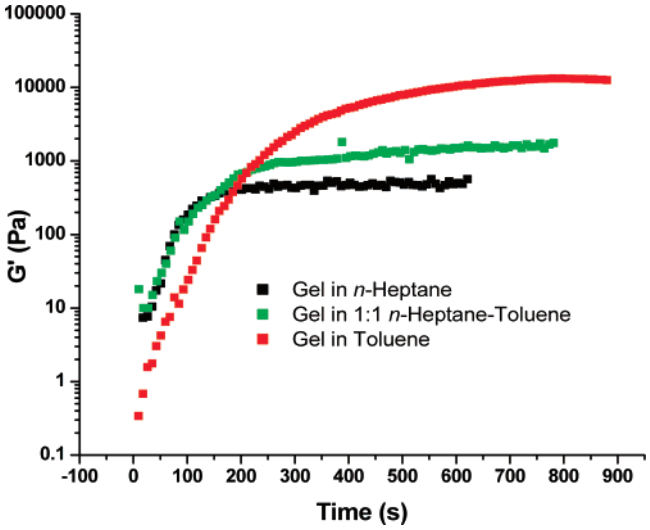

Figure 14. Time sweep experiments of gel recovery for the gels made in toluene, *n*-heptane, and 1:1 binary mixture of *n*-heptane−toluene with 40.5 mM of **1** at 25 °C.

It appears from Figure 13, in the frequency range of 0.01 to 550 rad/s, all the gels made from toluene, *n*-heptane, and 1:1 binary mixture of toluene and *n*-heptane, shows an almost constant elastic storage modulus G', which is always greater than the associated loss modulus G''. Nevertheless, over long-time scales (small frequencies of the applied stress), liquidlike flowing properties may prevail. Hence the G' and G'' are independent of the oscillation frequency, which is true for many other gels also. Also, the G' and G'' values of the toluene gel is much higher than that of *n*-heptane, while a gel prepared in their binary mixture possesses intermediate values. The complex viscosity decreased slowly and continuously with frequency, and the slope approached −1 in a log−log representation. This type of mechanical behavior is generally a characteristic observed in soft viscoelastic solids.[25]

Bulk rheological experiment can also exhibit the gel formation from the sol phase and subsequent growth of elastic properties. Figure 14 shows the result of a time-sweep experiment at 0.05% constant strain and 10 rad/s frequency during which the growth of the G' was monitored. The recovery of G' for *n*-heptane gel kinetically faster and took ∼160 s to reach saturation, whereas the toluene gel of **1** was found to form at slow kinetic rates and took ∼470 s. Gels made from the 1:1 binary mixture of *n*-heptane−toluene showed intermediate kinetic recovery of G'

with time. From the time-sweep experiment, it is clear that incorporation of toluene in the binary mixture of *n*-heptane−toluene makes the gelation kinetics much slower than that of gel made in *n*-heptane. The *n*-heptane solvent with its aliphatic chain interdigitates with the aliphatic chain of the gelators and induces faster fiber growth, while toluene being an aromatic hydrocarbon is unable to grow fibers at that fast rate. It is interesting that although the assembly in toluene is slower, it ultimately forms a stronger gel. This might indicate that although aliphatic solvents assist in the nucleation process by direct fiber−solvent interactions, the final network becomes more heavily solvated and hence weaker than the network formed in toluene, which will have a greater degree of fiber−fiber interactions.

4. Conclusions

This paper has for the first time addressed the aspect of gelation of solvent mixtures such as Heptol fractals by LMOG self-assembly and the following key points were demonstrated: A control of solvent composition led to gels with a reproducible XRD pattern and thermotropic and mechanical properties. Here, the composition of the solvent dictates the thickness of gel fibers. The gels made in *n*-heptane and toluene have completely different properties, and we suppose the gelator/solvent interactions are different in these gel. The toluene gel has one kind of morph present, whereas heptane gel shows polymorphism. Analysis of these morphs by XRD reveals the presence of two kinds of ordered layers. Gel of **1** in *n*-heptane is thermally more stable than that of toluene gel, and they behave differently at the transition temperature. The gels made in binary solvent mixture of toluene and *n*-heptane have intermediate thermal stability. In contrast, gel formed in toluene is more viscoelastic solid in nature than that of gel formed in *n*-heptane. Gels prepared in individual solvents or in their binary mixtures were found to be shear-thinning materials, and they all behave like soft viscoelastic materials. Most likely the polymorphism and dominance of fiber−solvent interaction over fiber−fiber interactions in *n*-heptane gel renders it less viscoelastic than toluene gel. The kinetics of gel formation provides an idea about the rate of fiber growth, and the aliphatic solvents facilitate the kinetics of fiber growth. Thus this study provides a framework for producing and characterization of gels with hydrocarbon fractals. It is important to point out that the methodology described herein for measuring and tuning the gel assembly should be applicable to other gelator systems; such information will be increasingly useful as the demand for designed, self-assembly system for achieving specific material property increases.

Acknowledgment. This work was supported by a grant from the Department of Biotechnology, New Delhi and FMC, India. We thank Prof. A. K. Sood and Dr. Rema for the access to rheology facility at the Physics Department. We also thank the Department of Science & Technology and the Institute Nanoscience Initiative for the SEM and AFM facility.

Supporting Information Available: Parts A and B of Figure S1 demonstrate enthalpy of gelation and solidification for toluene gels of **1**; Figure S2 depicts the DSC thermogram of different concentrations of **1** in *n*-heptane; Figure S3 shows a plot of temperature vs concentration of **1** in *n*-heptane; parts A and B of Figure S4 demonstrate enthalpy of gelation and solidification for *n*-heptane gel of **1**; rheological characterization of the gels have been discussed in Figures S5 and S6; Figures S7 and S8 show power law behavior of the gels. This information is available free of charge via the Internet at http://pubs.acs.org.

References and Notes

(1) Terech, P.; Weiss, R. G. *Chem. Rev.* **1997**, *97*, 3133−3159.
(2) Esch, J. H. v.; Feringa, B. L. *Angew. Chem., Int. Ed.* **2000**, *39*, 2263−2266.
(3) George, M.; Weiss, R. G. *Acc. Chem. Res.* **2006**, *39*, 489−497.
(4) Weiss, R. G.; Terech, P. *Molecular Gels: Materials with Self-Assembled Fibrillar Networks*; Springer: Dordrecht, 2006.
(5) Mukkamala, R.; Weiss, R. *Langmuir* **1996**, *12*, 1474−1482.
(6) Geiger, C.; Stanesau, M.; Chen, L.; Whitten, D. G. *Langmuir* **1999**, *15*, 2241−2245.
(7) Lu, L.; Cocker, T. M.; Bachman, R. E.; Weiss, R. G. *Langmuir* **2000**, *16*, 20−34.
(8) Jung, J. H.; Kobayashi, H.; Masuda, M.; Shimizu, T.; Shinkai, S. *J. Am. Chem. Soc.* **2001**, *123*, 8785−8789.
(9) Gu, W.; Lu, L.; Chapman, G. B.; Weiss, R. G. *Chem. Commun.* **1997**, 543−544.
(10) Oda, R., Huc, I., Candau, S. J. *Angew. Chem., Int. Ed.* **1998**, *37*, 2689−2691.
(11) Bhattacharya, S.; De, S., Subramanian, M. *J. Org. Chem.* **1998**, *63*, 7640−7651.
(12) (a) Bhattacharya, S.; De, S. *Langmuir* **1999**, *15*, 3400−3410. (b) Halder, J.; Aswal, V. K.; Goyal, P. S.; Bhattacharya, S. *Angew. Chem. Int. Ed.* **2001**, *40*, 1228−1232.
(13) Nakamura, K.; Shikata, T. *Langmuir* **2006**, *22*, 9853−9859.
(14) Amanokura, N.; Yoza, K.; Shinmori, H.; Shinkai, S.; Reinhoudt, D. N. *J. Chem. Soc., Perkin Trans.* **1998**, *2*, 2585−2592.
(15) Hafkamp, R. J. H.; Feiters, M. C.; Nolte, R. J. M. *J. Org. Chem.* **1999**, *64*, 412−426.
(16) Srivastava, A.; Ghorai, S.; Bhattacharjya, A.; Bhattacharya, S. *J. Org. Chem.* **2005**, *70*, 6574−6582.
(17) Bhattacharya, S.; Acharya, S. N. G. *Chem. Mater.* **1999**, *11*, 3504−3511.
(18) Bhattacharya, S.; Acharya, S. N. G. *Langmuir* **2000**, *16*, 87−97.
(19) Esch, J. H. v.; Kellogg, R. M.; Schryver. S. D.; Feringa, B. L. *Chem.−Eur. J.* **1997**, *3*, 1238−1243.
(20) Esch, J. H. v.; Schoonbeek, F.; Loos, M. d.; Kooijman, H.; Spek, A. L.; Kellogg, R. M.; Feringa, B. L. *Chem.−Eur. J.* **1999**, *5*, 937−950.
(21) Loos, M. d.; Esch, J. V.; Kellogg, R. M.; Feringa, B. L. *Angew. Chem., Int. Ed.* **2001**, *40*, 613−616.
(22) Abdallah, D. J.; Weiss, R. G. *Langmuir* **2000**, *16*, 352−355.
(23) Abdallah, D. J.; Sirchio, S. A.; Weiss, R. G. *Langmuir* **2000**, *16*, 7558−7561.
(24) Ragunathan, K. G.; Bhattacharya, S. *Chem. Phys. Lipids* **1995**, *77*, 13−23.
(25) Bhattacharya, S.; Acharya, S. N. G.; Raju, A. R. *Chem. Commun.* **1996**, 2101−2102.
(26) Bhattacharya, S.; Acharya, S. N. G. *Chem. Mater.* **1999**, *11*, 3121−3132.
(27) Hanabusa, K.; Tanaka, R.; Suzuki, M.; Kimura, M.; Shirai, H. *Adv. Mater.* **1997**, *9*, 1095−1097.
(28) Suzuki, M.; Sato, T.; Shirai, H.; Hanabusa, K. *New. J. Chem.* **2006**, *30*, 1184−1191.
(29) Hardy, J. G.; Hirst, A. R.; Ashworth, I.; Brennan, C.; Smith, D. K. *Tetrahedron* **2007**, *63*, 7397−7406.
(30) Gundert, G. M.; Klein, L.; Fischer, M.; Vögtle, F.; Heuzé, K.; Pozzo, J.-L.; Vallier, M.; Fages, F. *Angew. Chem., Int. Ed.* **2001**, *40*, 3164−3166.
(31) D'Aléo, A.; Pozzo, J.-L.; Fages, F.; Schmutz, M.; Gundert, G. M.; Vögtle, F.; Caplard, V.; Zinic, M. *Chem. Commun.* **2004**, 190−191.
(32) Kuroiwa, K.; Shibata, T.; Takada, A.; Nemoto, N.; Kimizuka, N. *J. Am. Chem. Soc.* **2004**, *126*, 2016−2021.
(33) Bhattacharya, S.; Krishnan-Ghosh, Y. *Chem. Commun.* **2001**, 185−186.
(34) Trivedi, D. R.; Ballabh, A.; Dastidar, P.; Ganguly, B. *Chem.−Eur. J.* **2004**, *10*, 5311−5322.
(35) Trivedi, D. R.; Dastidar, P. *Chem. Mater.* **2006**, *18*, 1470−1478.
(36) Bhattacharya, S.; Srivastava, A.; Pal, A. *Angew. Chem., Int. Ed.* **2006**, *45*, 2934−2937.
(37) Kimura, M.; Kobayashi, S.; Kuroda, T.; Hanabusa, K.; Shirai, H. *Adv. Mater.* **2004**, *16*, 335−338.
(38) Love, C. S.; Chechik, V.; Smith, D. K.; Wilson, K.; Ashworth, I.; Brennan, C. *Chem. Commun.* **2005**, 1971−1973.
(39) Suzuki, M.; Sato, T.; Shirai, H.; Hanabusa, K. *Chem. Commun.* **2006**, 377−379.
(40) Vemula, P. K.; John, G. *Chem. Commun.* **2006**, 2218−2220.
(41) Mitchell, D. L.; Speight, J. G. *Fuel* **1973**, *52*, 149−152.

(42) Andersen, S. I.; Keul, A.; Stenby, E. *Pet. Sci. Technol.* **1997**, *15*, 611−645.
(43) Andersen, S. I. *Fuel Sci. Technol. Int.* **1994**, *12*, 1551−1577.
(44) McLean, J. D.; Kilpatrick, P. K. *J. Colloid Interface Sci.* **1997**, *196*, 23−34.
(45) Fenistein, D.; Barre, L.; Broseta, D.; Espinat, D.; Livet, A.; Roux, J. N.; Scarsella, M. *Langmuir* **1998**, *14*, 1013−1020.
(46) Appaw, C.; Gilbert, R. D.; Khan, S. A.; Kadla, J. F. *Biomacromolecules* **2007**, *8*, 1541−1547.
(47) Daniel, C.; Alfano, D.; Guerra, G.; Musto, P. *Macromolecules* **2003**, *36*, 5742−5750.
(48) Pal, A.; Ghosh, Y. K.; Bhattacharya, S. *Tetrahedron* **2007**, *63*, 7334−7348.
(49) Zhu, G.; Dordick, J. S. *Chem. Mater.* **2006**, *18*, 5988−5995.
(50) Hirst, A. R.; Smith, D. K. *Langmuir* **2004**, *20*, 10851−10857.
(51) Guenet, J.-M., Eds. *Thermoreversible Gelation of Polymers and Biopolymers*; Academic Press: London, 1992.
(52) Terech, P.; Rossat, C.; Volino, F. *J. Colloid Interface Sci.* **2000**, *227*, 363−370.
(53) Li, H.; Yu, G. E.; Price, C.; Booth, C.; E. Hecht; Hoffmann, H. *Macromolecules* **1997**, *30*, 1347−1354.
(54) Brinksma, J.; Feringa, B. L.; Kellogg, R. M.; Vreeker, R.; Esch, J. v. *Langmuir* **2000**, *16*, 9249−9255.
(55) Moniruzzaman, M.; Sundararajan, P. R. *Langmuir* **2005**, *21*, 3802−3807.
(56) Larson, R. G. *The Structure and Rheology of Complex Fluids*; Oxford University Press: New York, 1999.
(57) Bychuk, O.; Shaughnessy, B. O. *Phys. Rev. Lett.* **1995**, *74*, 1795−1798.
(58) Menger, F. M.; Yamasaki, Y.; Catlin, K. K.; Nishimi, T. *Angew. Chem., Int. Ed.* **1995**, *34*, 585−586.
(59) Menger, F. M.; Peresypkin, A. V. *J. Am. Chem. Soc.* **2003**, *125*, 5340−5345.
(60) Menger, F. M.; Caran, K. L. *J. Am. Chem. Soc.* **2000**, *122*, 11679−11691.
(61) Jover, A.; Meijide, F.; Nunez, E. R.; Tato, J. V. *Langmuir* **2002**, *18*, 987−991.
(62) Shih, W.-H.; Shih, W. Y.; Kim, S.-I.; Liu, J.; Aksay, I. A. *Phys. Rev. A* **1990**, *42*, 4772−4779.
(63) Terech, P.; Pasquier, D.; Bordas, V.; Rossat, C. *Langmuir* **2000**, *16*, 4485−4494.